24 GHz Graphene Patch Antenna Array

Varindra Kumar

Department of Engineering, University of Cambridge, Cambridge, CB2 1PZ, UK
Varindra@ieee.org

Abstract ─ The discovery of Graphene has created new applications for the next generation electronics due to its electrical characteristic. A compact patch antenna with graphene as conducting media has been designed for wearable, medical and consumer electronics application at 24 GHz. The patch has a dimension of 5x5 mm and is designed over 0.254 mm thick roger material. The antenna has been combined to make it an array form for increasing its gain while various antenna parameters have been obtained for its comparison with copper conductive patch. The ground patch is made of Perfect Electric Conductor (PEC) in both cases. Various parametric results show that graphene patch similar to copper patch provides a comparable return loss and VSWR although there has been observed some decrease in its gain and efficiency and an increase in its bandwidth. Thus, graphene can be a good alternative to copper conductive patch within higher GHz and THz frequency range.

Index Terms ─ 24 GHz, antenna, array, graphene, patch.

I. INTRODUCTION

The last few years has seen an increase in the arrival of small and portable electronics for its wide-ranging applications from IoT, consumer, medical and wearable electronics. In order to make these electronics smaller and robust, every component of these devices need to be small and low profile while providing similar output. Antenna being the communication component across these devices needs to be small while providing good performance. An array of the antenna can provide an increase in its parametric values with increasing gain and radiation efficiency in certain direction while suppressing these values in undesired direction [1-5]. Various researchers in the past have proposed the design of an array antenna with traditional conducting media such as copper, silver etc to increase the gain and bandwidth but very few have designed an array antenna with graphene conductive media [6-7] at low GHz frequency range. Graphene [8] is hexagonally arranged honeycombed lattice structure with high mobility (8000 cm^2/V) [8-9], thermal conductivity of 5000 W/m/K [8-9], mechanical strength [8-9] and noticeable flexibility [10]. Recently graphene as a material has become quite popular and has provided many applications in microwave to mm-wave domain [11-12]. The application in microwave and mm wave is often associated with high propagation and penetration losses. However, this paper proposes the graphene application in GHz communication with an array to increase the signal strength, gain and directivity. The low conductivity of the graphene flake at lower GHz frequency range requires a layer combination where the conductivity can be increased with an increase in number of layers although the constraint lies in the manufacturing of a thick layer of graphene flake [13-15].

II. ANTENNA DESIGN

Microstrip patch antenna has a conductive patch laid over a substrate with a metallic conductor underneath to provide a ground plane. The performance of a patch such as resonant frequency, gain, directivity, radiation and bandwidth depends on the patch dimension and size, substrate type and feed. The effective permittivity of the substrate can be defined using (1) [16] while the patch dimension can be obtained using its required resonant frequency after a calculation from (2-7) [16] with the assumption 'W' width being greater than substrate thickness 'h':

$$\varepsilon_{reff} = \frac{\varepsilon_r+1}{2} + \frac{\varepsilon_r-1}{2}\frac{1}{\sqrt{1+\frac{12h}{W}}}, \tag{1}$$

$$W = \frac{c}{2f_o\sqrt{\frac{\varepsilon_r+1}{2}}}, \tag{2}$$

$$L_{eff} = \frac{c}{2f_o\sqrt{\varepsilon_{reff}}}, \tag{3}$$

$$\Delta L = 0.412h\frac{\left(\varepsilon_{reff}+0.3\right)\left(\frac{W}{h}+0.264\right)}{\left(\varepsilon_{reff}-0.258\right)\left(\frac{W}{h}+0.8\right)}, \tag{4}$$

$$L = L_{eff} - 2\Delta L, \tag{5}$$

$$L_g = 6h + L, \tag{6}$$

Submitted On: February 22, 2018
Accepted On: December 25, 2018

$$W_g = 6h + W. \quad (7)$$

The proposed antenna is a rectangular radiation patch with a feeding patch structure of 50Ω characteristic impedance and is shown in Fig. 1. The antenna designs have been converted into an array form and are shown in Figs. 2-4, while Fig. 5 shows the stack-up of the design [17]. The conducting patch (3.4 mm x 2.38 mm) has been designed using copper and graphene media with roger material as substrate (dielectric constant ϵ_r = 6.15 and tan δ = 0.002) with dimensional size of 10 mm x 10 mm and PEC at its ground layer with dimensional size of 10 mm x 10 mm. The patch and its ground layer have a thickness of 0.01 mm while the substrate is 0.254 mm thick. The patch is excited through a feed with the dimension of 0.32 mm x 4.71 mm x 0.01 mm.

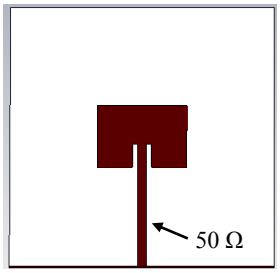

Fig. 1. Patch antenna.

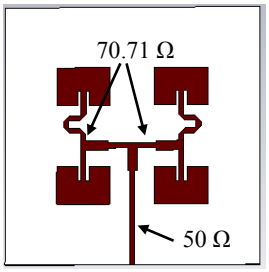

Fig. 2. 2x2 Patch antenna.

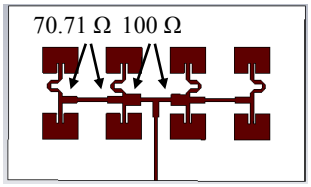

Fig. 3. 2x4 Patch antenna.

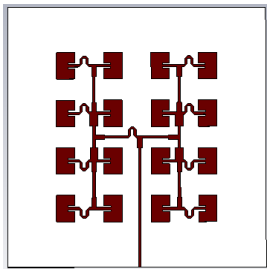

Fig. 4. 4x4 Patch antenna.

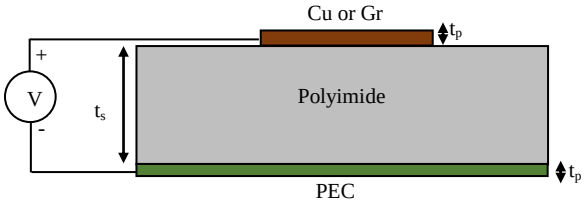

Fig. 5. Copper/graphene patch antenna (side view).

III. GRAPHENE AND ITS CONDUCTIVITY

The graphene surface conductivity arises from the Kubo formula [18-19] in the absence of an external electric and magnetic field; however is frequency dependent and is represented as a complex number. The first term of (8) represents intraband conductivity while the second term represents interband conductivity. Various parameters ω, μ_C, τ, T, e and ħ of the following equations (8-16) are defined by the operating frequency, external chemical bias to a graphene structure, carrier scattering time constant (1/τ defines carrier scattering rate), room temperature, electronic constant and reduced Planck's constant respectively. Similarly, k_B, $f_d(\epsilon)$, V_f and n_s represents the Boltzmann constant, Fermi Dirac distribution function, Fermi velocity (10^6 m/s) and electron mobility respectively:

$$\sigma(\omega,\mu_C,\tau,T) = \frac{je^2/\pi\hbar^2}{\omega - j(2/\tau)} \times \int_0^\infty \varepsilon \left[\frac{\partial f_d(\varepsilon)}{\partial \varepsilon} - \frac{\partial f_d(-\varepsilon)}{\partial \varepsilon} \right] d\varepsilon + je^2/\pi\hbar^2(\omega - j(2/\tau) \times \int_0^\infty \frac{f_d(\varepsilon) - f_d(-\varepsilon)}{(\omega - j(2/\tau))^2 - 4(\varepsilon/\hbar)^2} d\varepsilon, \quad (8)$$

$$f_d(\varepsilon) = \left[1 + e^{\frac{\varepsilon + |\mu_C|}{k_B T}} \right]^{-1}, \quad (9)$$

$$n_s = \frac{2}{\pi\hbar^2 V_f^2} \int_0^\infty \varepsilon \left[\begin{matrix} f_d(\varepsilon - \mu_C) - \\ f_d(\varepsilon + \mu_C) \end{matrix} \right] d\varepsilon, \quad (10)$$

$$\tau = \frac{\mu \mu_C}{e V_f^2}, \quad (11)$$

$$\mu_C = \sqrt{\pi\hbar^2 V_f^2 n_s}, \quad (12)$$

$$n_s = \frac{2}{\pi\hbar^2 V_f^2} (k_B T)^2 \left(e^{\frac{2\mu_C}{k_B T}} - 1 \right), \quad (13)$$

$$\sigma_{\text{int ra}}(\omega,\mu_C,\tau,T) = j \frac{8\sigma_0 k_B T/h}{\omega - j2/\tau} \times \left[\frac{\mu_C}{k_B T} + 2\ln\left(e^{-\frac{\mu_C}{k_B T}} + 1 \right) \right], \quad (14)$$

$$\sigma_{\text{int er}}(\omega,\mu_C,\tau,T) = -j \frac{\sigma_0}{\pi} \times \left[\frac{2|\mu_C| - (\omega - j2/\tau)\hbar}{2|\mu_C| + (\omega - j2/\tau)\hbar} \right], \quad (15)$$

$$\delta = \sqrt{\frac{2}{\omega\mu\sigma}}. \quad (16)$$

Fermi Dirac function and carrier mobility can be represented using (9) and (10) while scattering time constant and chemical bias are represented using (11) and (12). Solving (10) with the help of (9), the carrier mobility as defined in (13) can be obtained. Based on (14) and (15), a normalized conductivity plot with the chemical potential ranging from 0.1 eV to 1.1 eV for a graphene flake within the GHz - THz frequency range has been obtained and plotted using Matlab as shown in Fig. 6. The conductivity has been normalized here to its static conductivity $\sigma_0 = e^2/(4\hbar)$ for its plot. The graphene has a lattice structure with extremely thin layer of height (δ = 0.334 nm) and hence it can be considered as a two dimensional crystalline structure. For the electromagnetic simulation, the lattice structure's minimum thickness δ is selected such that the electromagnetic field distribution can see the thickness of the graphene and a wave propagation can occur. Hence the graphene conductivity can be

expressed as volumetric conductivity with $\sigma_v = \sigma_s/\delta$. With a layer of graphene flake to create a patch (thickness tp) in antenna design, the effective surface conductivity in its simplified form can be represented as $\sigma = tp \times \sigma_v$. Here N-layered graphene with tp/δ has been assumed to have the same relaxation time and fermi energy for its simplicity.

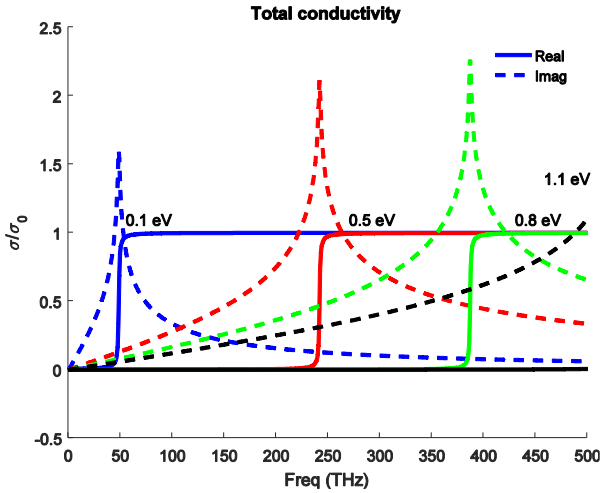

Fig. 6. Normalized total conductivity of Graphene.

IV. RESULTS AND DISCUSSION

A full field solver tool, CST Microwave studio [20] is used for the design and simulation of the antenna and Matlab is used to plot the data within the frequency band from 20 GHz to 28 GHz.

Figures 7-10 show the S11 parameter comparison for the copper and graphene patch for its configurations 1x1, 2x2, 2x4 and 4x4 while a comparison of its gain for the patch array with copper and graphene media has been shown in Figs. 11-14. As shown in these figures, the resonance frequency of the copper patch compares well with the graphene patch at around 24 GHz resonance with 0.1 eV DC bias. The gain behavior as shown in Figs. 11-14 shows that with an increase in the number of patch element forming an array increases the gain. The patch with graphene media shows slightly lesser gain while still providing enough performance for its antenna application.

Using the transmission line theory, various equations to obtain antenna parameters for a rectangular patch lying in x-y plane (perpendicular to z- axis) with length 'L' and width 'W' using simple formulas can be obtained and are defined in (17-25) [21-22]. As the reflection coefficient at its load can be defined using (17), the reflection coefficient as a function of x along its length (or y along its width) can be obtained using (18), while the Voltage Standing Wave Ratio (VSWR) can be obtained using (19).

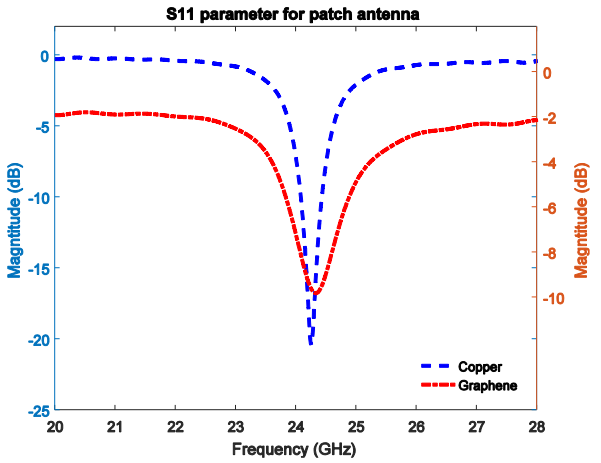

Fig. 7. S11 parameter comparison for Copper and Graphene - 1x1 patch.

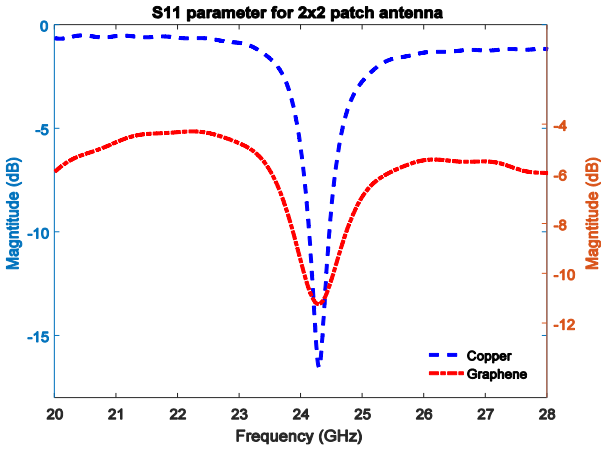

Fig. 8. S11 parameter comparison for Copper and Graphene - 2x2 patch.

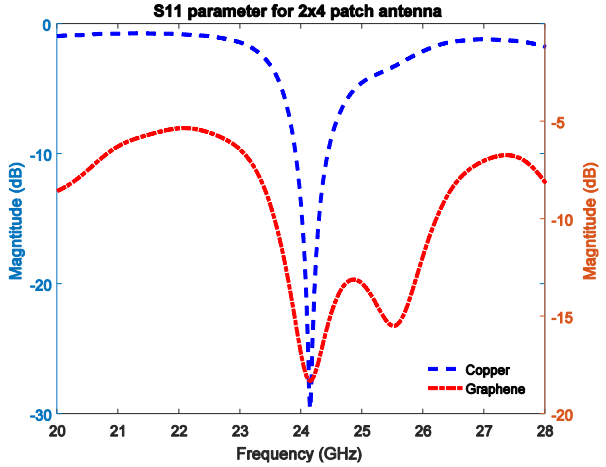

Fig. 9. S11 parameter comparison for Copper and Graphene - 2x4 patch.

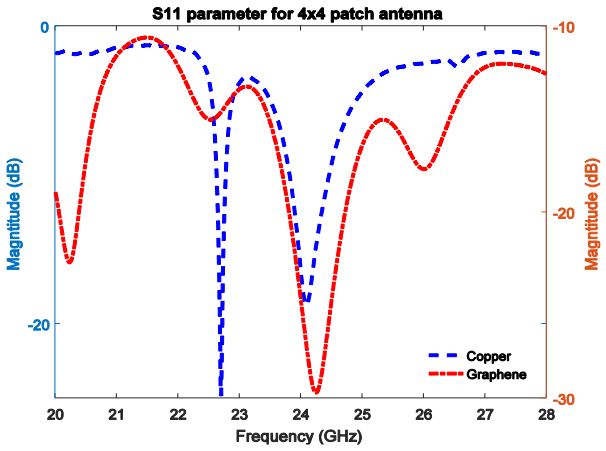

Fig. 10. S11 parameter comparison for Copper and Graphene - 4x4 patch.

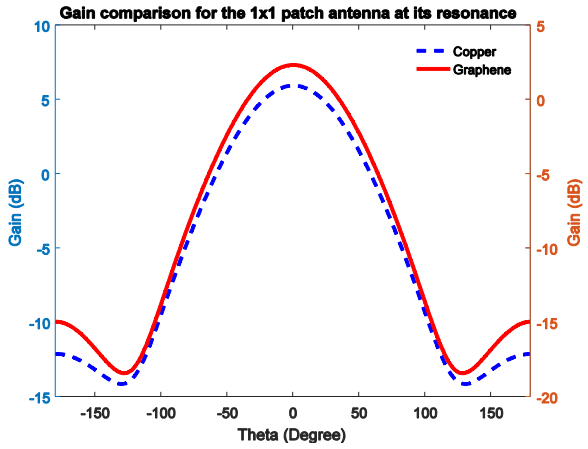

Fig. 11. Gain comparison for 1x1 patch antenna.

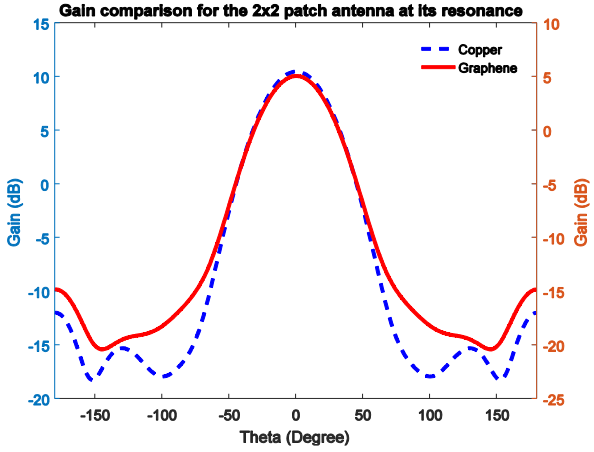

Fig. 12. Gain comparison for 2x2 patch antenna.

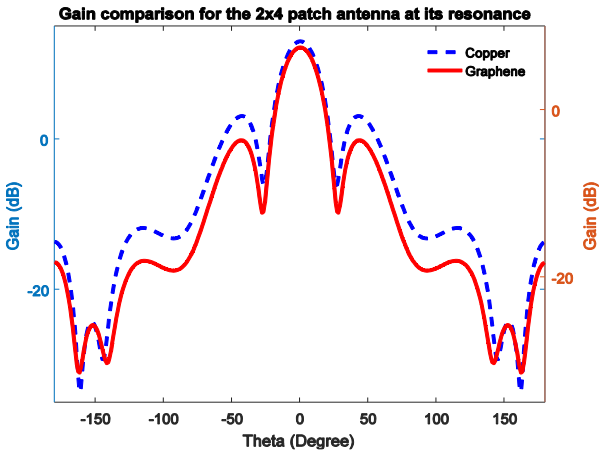

Fig. 13. Gain comparison for 2x4 patch antenna.

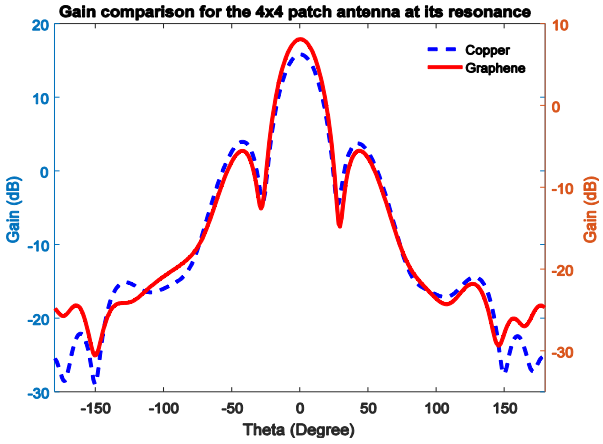

Fig. 14. Gain comparison for 4x4 patch antenna.

The resonance frequency of a rectangular patch with length 'L' and width 'W' in general is dependent on the mode of its excitation and can be defined by its TE, TM, TEM mode based on the integer values of m and n as in (20) while the bandwidth (BW) as in (21) can be obtained with its upper and lower -10dB crossing point. Similarly based on the dielectric and conductor loss of a conductive patch over a substrate can provide a relationship for gain and directivity for its radiation efficiency and can be defined using (22) while the normalized electromagnetic fields with respect to peak field at its corner can be obtained using (23), (24), and (25). Here $k_0 = 2\pi/\lambda$, where λ is the wavelength of the excited frequency of operation:

$$\Gamma_L = \frac{Z_L - Z_o}{Z_L + Z_o}, \tag{17}$$

$$\Gamma(x) = \Gamma_L e^{2j\beta x}, \tag{18}$$

$$\text{VSWR} = \frac{1+|\Gamma(x)|}{1-|\Gamma(x)|}, \tag{19}$$

$$f_O = \frac{c}{2\sqrt{\varepsilon_r}}\left[\left(\frac{m}{L}\right)^2 + \left(\frac{n}{W}\right)^2\right]^{1/2}, \tag{20}$$

$$\text{BW} = (f_H - f_L), \tag{21}$$

$$G(\theta,\varphi) = \delta_e D(\theta,\varphi), \tag{22}$$

$$E_z = \cos\left(\frac{m\pi x}{L}\right)\cos\left(\frac{n\pi y}{W}\right), \tag{23}$$

$$H_x = -\frac{j\omega\varepsilon_0}{k_0^2}\frac{n\pi}{W}\cos\left(\frac{m\pi x}{L}\right)\sin\left(\frac{n\pi y}{W}\right), \tag{24}$$

$$H_y = \frac{j\omega\varepsilon_0}{k_0^2}\frac{m\pi}{L}\sin\left(\frac{m\pi x}{L}\right)\cos\left(\frac{n\pi y}{W}\right). \tag{25}$$

The radiation field of an array at a far point as defined in (26) can be assumed as a weighted sum of the radiation due to an array of elements, with a consideration of the phase for individual element, similarly the gain can be obtained as the weighted sum of individual array element [23]. Here r_n represents the (x, y, z) distance of the calculation point from the individual element of the array:

$$R_{sum}(x_f, y_f, z_f) = \sum_{n=1}^{N} R_n(x_f, y_f, z_f) \times w_n \frac{e^{-jkr_n}}{r_n}. \tag{26}$$

A far-field radiation diagram for various patch antenna has been obtained and are shown in Figs. 15-22. As shown here, Figs. 15-18 show the radiation pattern for the copper patch for its various array structures. With an increase in array dimension, the directivity of the patch shows an increase. Similarly, Figs. 19-22 show the radiation pattern for the graphene patch for its various array structures. A comparison of the radiation pattern for copper and graphene patch shows that the directivity of the graphene closely follows the corresponding pattern of copper patch.

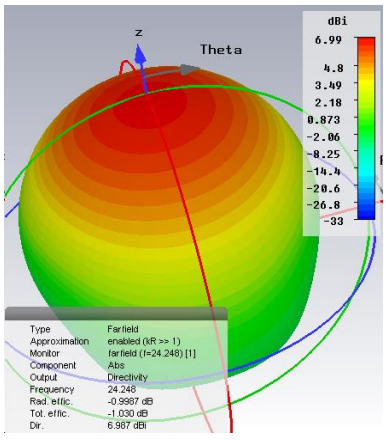

Fig. 15. Radiation diagram for 1x1 Copper patch.

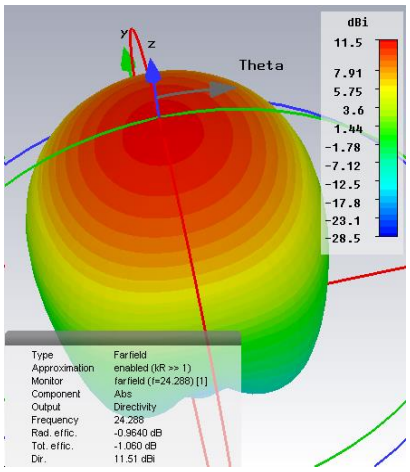

Fig. 16. Radiation diagram for 2x2 Copper patch.

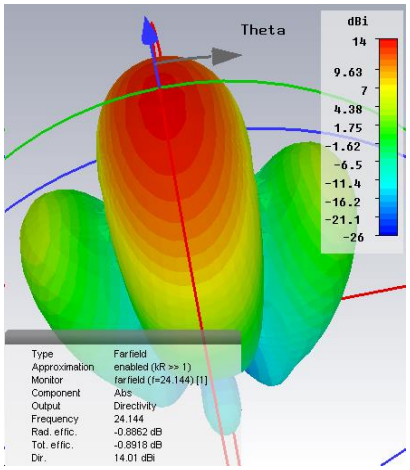

Fig. 17. Radiation diagram for 2x4 Copper patch.

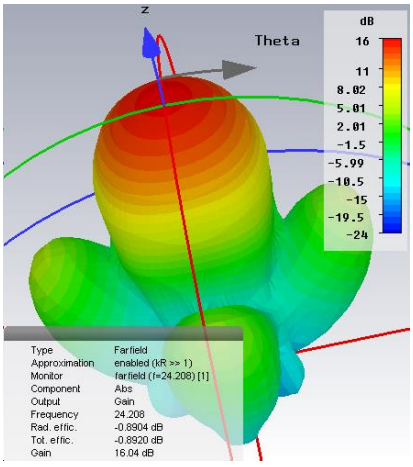

Fig. 18. Radiation diagram for 4x4 Copper patch.

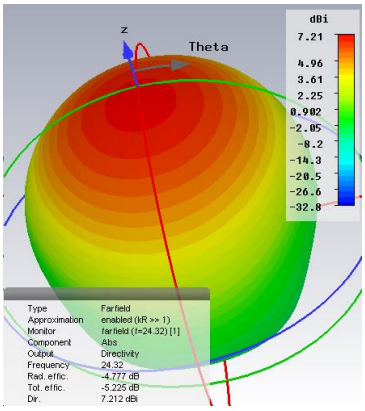

Fig. 19. Radiation diagram for 1x1 Graphene patch.

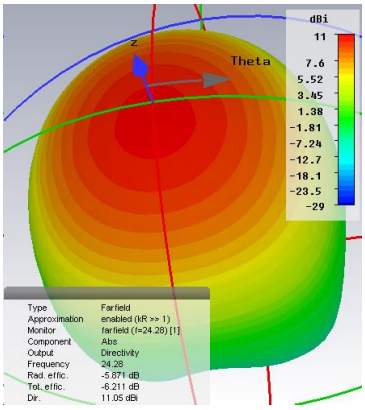

Fig. 20. Radiation diagram for 2x2 Graphene patch.

Table 1 provides a comparison of various antenna parameters for copper and graphene conductive patch in its array form such as resonant frequency, VSWR, return loss, Directivity, Gain, Directivity and radiation efficiency. Although radiation efficiency is lower for the graphene media, these patch elements can still be used for antenna application.

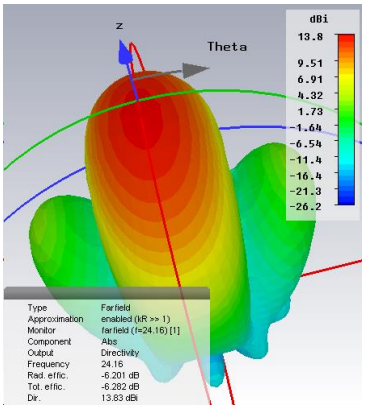

Fig. 21. Radiation diagram for 2x4 Graphene patch.

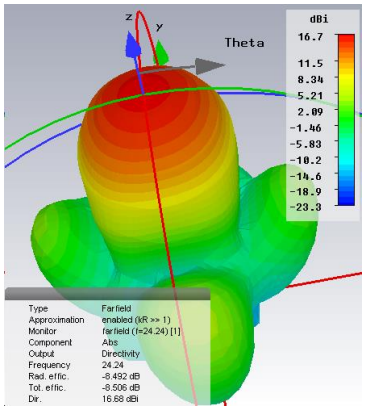

Fig. 22. Radiation diagram for 4x4 Graphene patch.

Table 1: Antenna parametric comparison for graphene and copper

	Conductor	Freq. (GHz)	Bandwidth (MHz)	S11 (dB)	VSWR
1x1	Copper	24.248	348	-20.37	1.21
	Graphene	24.32	0	-10.0	1.96
2x2	Copper	24.288	327	-16.51	1.35
	Graphene	24.28	47	-11.21	1.76
2x4	Copper	24.144	523	-29.58	1.07
	Graphene	24.16	2640	-18.29	1.28
4x4	Copper	24.208	613	-27.43	1.09
	Graphene	24.24	8000	-29.69	1.07

	Conductor	Directivity (dBi)	Angular Width (°)	Gain (dB)	Radiation Eff. (%)
1x1	Copper	6.99	36.1	5.99	79.46
	Graphene	7.21	32.7	2.43	33.29
2x2	Copper	11.51	21.9	10.55	80.09
	Graphene	11.05	22.5	5.18	25.88
2x4	Copper	14.01	22.0	13.12	81.54
	Graphene	13.83	22.7	7.63	23.98
4x4	Copper	16.93	16.6	16.04	81.46
	Graphene	16.68	15.2	8.19	14.15

V. SPICE EQUIVALENT

A Spice equivalent circuit for the 4x4 graphene patch antenna has been obtained using ADS tool and the obtained S11 parameter has been compared with the S11 parameter obtained from CST tool as shown in Figs. 24 and 25. Figure 23 shows the obtained 7 stage RLC ladder circuit with its parametric values and is shown in Table 2. A transfer function representing zeros and poles can be used to define the S11 parameter of the patch and using the transmission line theory, the complete patch can be represented using a [RLGC] matrix and after some optimization using ADS tool, its equivalence can be obtained:

$$H(S) = \sum_{i=1}^{N} \left(\frac{Z_i}{S - P_i} \right) + d. \qquad (27)$$

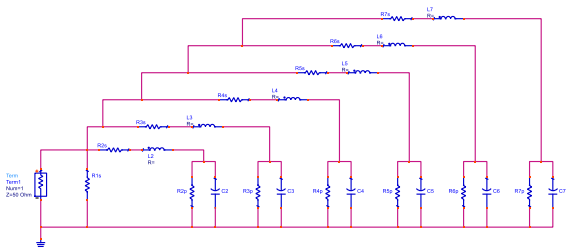

Fig. 23. S11 parameter Spice circuit for 4x4 graphene patch.

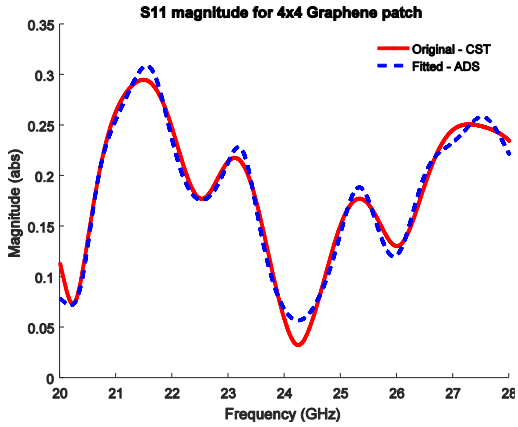

Fig. 24. S11 original and fitted magnitude for Graphene Patch.

Table 2: RLC parameters for the spice circuit

RLC Parameters	Stage 1	Stage 2
R_s(i) (Ω)	61.314446338757	-6859.00485872161
L(i) (nH)		38.1581758308437
C(i) (fF)		0.528633569251257
Rp(i) (kΩ)		10.2896757212470

RLC Parameters	Stage 3
R_s(i) (Ω)	1019.41363184957
L(i) (nH)	11.5125787550172
C(i) (fF)	2.30779927956048
Rp(i) (kΩ)	-5.16417026902054

RLC Parameters	Stage 4	Stage 5
R_s(i) (Ω)	1262.47629042827	2762.15685319658
L(i) (nH)	12.9777407332746	-20.1487936026862
C(i) (fF)	2.76783830152791	-1.20537208494751
Rp(i) (kΩ)	-3.88857348344465	-5.79145334311434

RLC Parameters	Stage 6	Stage 7
R_s(i) (Ω)	-1475.59209098543	-1977.56405676355
L(i) (nH)	12.8363609393114	-13.3267861687389
C(i) (fF)	1.90704567947197	-1.63138998131753
Rp(i) (kΩ)	4.36159370923036	4.35594530526759

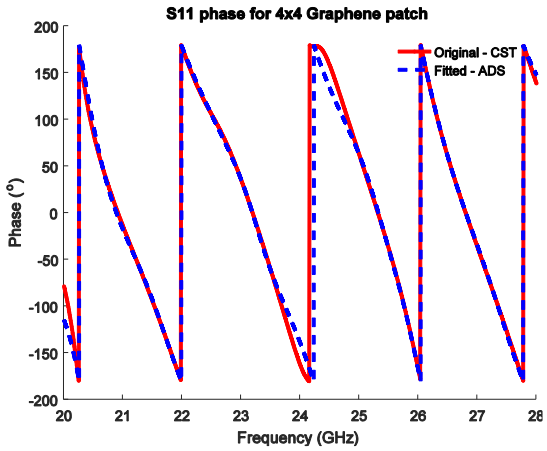

Fig. 25. S11 original and fitted phase for Graphene Patch.

VI. CONCLUSION

Here graphene-based array antenna for the medical and wearable electronics applications and operating at 24 GHz has been proposed and its result has been compared with copper conducting media. The simulation results show that the gain and radiation pattern of the graphene patch antenna compares reasonably well to a conventional copper patch antenna. This shows promising results for the graphene material in the upper GHz frequency range. A Spice equivalence with RLGC parameters of the 4x4 graphene patch for its S11 parameter has been obtained for its inclusion in a traditional spice solver tool and its result has been compared with a 3D field solver result.

ACKNOWLEDGMENT

The author would like to acknowledge the funding and support received from the Department of Engineering, University of Cambridge.

REFERENCES

[1] G. Casu, C. Moraru, and A. Kovacs, "Design and implementation of microstrip patch antenna array," *2014 10th International Conference on Communications (COMM)*, Bucharest, pp. 1-4, Doi: 10.1109/ICComm.2014.6866738, 2014.

[2] N. Ghassemi and K. Wu, "High-efficient patch antenna array for E-band gigabyte point-to-point wireless services," *IEEE Antennas and Wireless Propagation Letters*, vol. 11, pp. 1261-1264, Doi: 10.1109/LAWP.2012.2224087, 2012.

[3] Y. J. Cheng, Y. X. Guo, and Z. Q. Liu, "W-Band large-scale high-gain planar integrated antenna array," *IEEE Transactions on Antennas and Propagation*, vol. 62, pp. 3370-3373, Doi: 10.1109/TAP.2014.2310483, 2014.

[4] J. Kim II, B. M. Lee, and Y. J. Yoon, "Wideband printed dipole antenna for multiple wireless serv-

ices," *Proceedings RAWCON 2001, 2001 IEEE Radio and Wireless Conference (Cat.No.01EX514)*, Waltham, MA, pp. 153-156, Doi: 10.1109/RAWCON. 2001.947575, 2001.

[5] J. D. Kraus, R. J. Marhefka, and A. S. Khan, *Antennas for All Applications*. Tata McGraw-Hill, 3rd ed., New Delhi, ISBN-10: 0-07-060185-2, 2006.

[6] S. N. H. Sa'don, M. R. Kamarudin, F. Ahmad, M. Jusoh, and H. A. Majid, "Graphene array antenna for 5G applications," *Appl. Phys. Mater. Sci. Process*, vol. 123, pp. 1-4, Doi: 10.1007/s00339-016-0749-5, 2017.

[7] M. Donelli and G. Oliveri, "Design of tunable graphene-based antenna arrays for microwave applications," *Proc. IEEE APSURSI*, Memphis, TN, USA, pp. 6-12. Doi: 10.1109/aps.2014.6904782, 2014.

[8] A. K. Geim and K. S. Novoselov, "The rise of graphene," *Nature Mater.*, vol. 6, pp. 183-191, Doi: 10.1038/nmat1849, 2007.

[9] K. S. Novoselov, A. K. Geim, S. V. Morozov, D. Jiang, Y. Zhang, S. V. Dubonos, I. V. Grigorieva, and A. A. Firsov, "Electric field effect in atomically thin carbon films," *Science*, vol. 306, pp. 666-669, Doi: 10.1126/science.1102896, 2004.

[10] R. Song, Q. Wang, B. Mao, Z. Wang, D. Tang, B. Zhang, J. Zhang, C. Liu, D. He, Z. Wu, and S. Mu, "Flexible radio films with high conductivity for radio frequency antennas," *Carbon*, vol. 130, pp. 164-169, Doi: 10.1016/j.carbon.2018.01.019, 2018.

[11] J. H. Warner, F. Schaffel, M. Rummeli, and A. Bachmatiuk, *Graphene Fundamentals and Emergent Applications*. Elsevier, Oxford, 2013.

[12] M. Bozzi, L. Pierantoni, and S. Bellucci, "Applications of graphene at microwave frequencies," *Radioengineering*, vol. 24, pp. 661-669, Doi: 10.13164/ re.2015.0661, 2015.

[13] Q. Zheng and J.-K. Kim, *Graphene for Transparent Conductors: Synthesis, Properties and Applications*, Springer-Verlag, New York, Doi: 10.1007/978-1-4939-2769-2, 2015.

[14] Y. Wang, S. W. Tong, X. F. Xu, B. Ozyilmaz, and K. P. Loh, "Interface engineering of layer-by-layer stacked graphene anodes for high-performance organic solar cells," *Adv. Mater.*, vol. 23, pp. 1514-1518, Doi: 10.1002/adma.201003673, 2011.

[15] R. R. Nair, P. Blake, A. N. Grigorenko, K. S. Novoselov, T. J. Booth, T. Stauber, N. M. R. Peres, and A. K. Geim, "Fine structure constant defines visual transparency of graphene," *Science*, vol. 320, pp. 1308, Doi: 10.1126/science.1156965, 2008.

[16] C. A. Balanis, *Antenna Theory: Analysis and Design*. John Wiley & Sons, New Jersey, USA, 2005.

[17] T. Stauber, N. M. Peres, and A. K. Geim, "Optical conductivity of graphene in the visible region of the spectrum," *Physical Review B*, vol. 78, pp. 085432, Doi: 10.1103/PhysRevB.78.085432, 2008.

[18] S. A. Mikhailov and K. Ziegler, "New electromagnetic mode in graphene," *Physical Review Letters*, vol. 99, pp. 016803, Doi: 10.1103/ PhysRevLett.99.016803, 2007.

[19] G. W. Hanson, "Dyadic Green's functions and guided surface waves for a surface conductivity model of graphene," *J. Appl. Phys.*, vol. 103, pp. 064302, Doi: 10.1063/1.2891452, 2008.

[20] CST Microwave Studio, Computer Simulation Technology, Framingham, MA [online]. http://www.cst.com, 2019.

[21] S. Bae, H. Kim, Y. Lee, X. Xu, J. S. Park, Y. Zheng, J. Balakrishnan, T. Lei, H. R. Kim, Y. I. Song, Y. J. Kim, K. S. Kim, B. Ozyilmaz, J. H. Ahn, B. H. Hong, and S. Iijima, "Roll-to-roll production of 30-inch graphene films for transparent electrodes," *Nat. Nanotechnol.*, vol. 5, pp. 574-578, Doi: 10.1038/nnano.2010.132, 2010.

[22] Y. Huang and K. Boyle, *Antenna from Theory to Practice*. 1st ed., Wiley & Sons Ltd., New Delhi, ISBN: 978-0-470-51028-5, 2006.

[23] J. R. James, P. S. Hall, and C. Wood, *Microstrip Antenna Theory and Design*. Peter Peregrinus Ltd, London, ISBN: 0-86341-088, 1986.

[24] R. J. Mailloux, *Phased Array Antenna Handbook*. 2nd ed., Artech house, Norwood, MA, ISBN: 1-58053-689-1, 2005.

Varindra Kumar has obtained his Bachelor of Engineering in Electronics from National Institute of Technology (Formerly REC) Rourkela and Master of Technology in Electronics and Communication Engineering from Indian Institute of Technology, Varanasi (Formerly IT BHU). Subsequently after working across various electronics design companies, he joined for Ph.D. at the University of Nottingham in EMC Macromodeling. After finishing his Ph.D. in the year 2014, he is working as Postdoc Research Associate at the Department of Engineering, University of Cambridge. His research interest lies in electronics design, microprocessor architecture, sensor design, wearable electronics, electromagnetic and antenna design etc.